PCCP

PAPER

View Article Online
View Journal | View Issue

Cite this: *Phys. Chem. Chem. Phys.*, 2017, **19**, 21350

Catalysis by solvation rather than the desolvation effect: exploring the catalytic efficiency of SAM-dependent chlorinase†

Edson Araújo,[a] Anderson H. Lima[b] and Jerônimo Lameira *[a]

Received 30th April 2017,
Accepted 14th July 2017

DOI: 10.1039/c7cp02811c

rsc.li/pccp

Chlorinase SalL halogenate *S*-adenosyl-L-methionine (SAM) reacts with chloride to generate 5′-chloro-5′-deoxyadenosine and L-methionine through a nucleophilic substitution mechanism. Although it is known that chlorinase enhances the rate of reaction by a factor of 1.2×10^{17} fold, it is not entirely clear how this is accomplished. The search for the origin of the catalysis of chlorinase and other enzymes has led to a desolvation hypothesis. In the present work, we have used well defined computational simulations in order to evaluate the origin of the catalytic efficiency of chlorinase. The results demonstrate that the catalytic effect of chlorinase is associated with the fact that Cl^- is "solvated" by the protein more than by the reference solution reaction, which is not in accordance with proposed catalysis by desolvation. It is found that chlorinase SalL active sites provide electrostatic stabilization of the transition state which is the origin of its catalytic effect.

Introduction

Adenosyl-chloride synthase or chlorinase SalL is involved in chloride insertion into the marine natural product salinosporamide A from *Salinospora tropica*.[1] This enzyme mediates a nucleophilic reaction between SAM and chloride ions to generate 5′-chloro-5′-deoxyadenosine (5′-ClDA) and L-methionine (see Fig. 1). Chlorinase SalL catalyzes the first committed step in the biosynthesis of salinosporamide A, a compound that displays 20S proteasome inhibition and has entered clinical trials for multiple myeloma and other cancer treatments.[2] High-resolution crystal structures of SalL and active site mutants in complex with substrates and products support the S_N2 nucleophilic substitution mechanism and further illuminate halide specificity in this newly discovered halogenase family.[1] In light of the biological importance of this enzyme, it is important to study the molecular origin of its catalytic power.

In a recent contribution, Wolfenden and coworkers have provided very useful information on the catalysis of alkyl transfer from SAM to halide ions,[3] where they have suggested that SAM dependent halide alkylating enzymes catalyze the reaction by the "desolvation" effect.[4] The desolvation proposal suggests that an enzyme enhances the reactivity of a polar or a charged reacting fragment by shifting it from a polar environment to its nonpolar cavity, resulting in reactant destabilization relative to a less polar transition state.[5] We note, however, that computational works[6–8] have indicated that there is no justification for this hypothesis, since the reduction of the activation barrier appears to result mainly from electrostatic interactions that 'solvate' the reactant state (RS) and the transition state (TS) in the protein more than in solution.[9,10]

Recently, we have used a free energy surface and the quantum mechanics/molecular mechanics (QM/MM) approach[11] to investigate biomolecular systems with an emphasis on enzymatic reactions.[7,12–14] In the present work, we evaluated the activation free energy for SAM chlorination in both the protein environment and aqueous solution to clarify whether chlorinase can catalyze the formation of 5′-ClDA and L-methionine (Fig. 1) by desolvation or electrostatic preorganization. Our analysis is supported by the electrostatic preorganization effect[10] and the idea that an enzyme replaces water by acting as a strong "solvent".[6]

Methods

The EVB method

In this work, we have used the empirical valence bond (EVB) method,[15] to compute the free energy activation barriers for the reaction catalyzed by chlorinase. In this method, the reaction is described by diabatic states that correspond to classical valence bond (VB) structures which represent the reactants (or intermediate) and product states, where the reaction free energy profile is calculated on the ground state energy surface, E_g. The ground

[a] *Institute of Biological Sciences, Federal University of Pará, 66075-110, Belém, PA, Brazil. E-mail: lameira@ufpa.br; Tel: +55 91-32018235*
[b] *Institute of Exact and Natural Sciences, Federal University of Pará, 66075-110, Belém, PA, Brazil*

† Electronic supplementary information (ESI) available. See DOI: 10.1039/c7cp02811c

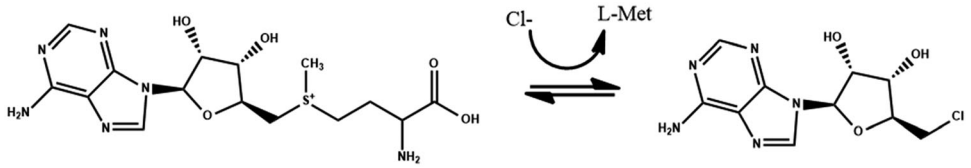

Fig. 1 Reaction involving SAM and chloride ions to generate 5′-ClDA and L-Met catalyzed by SalL methyl transferase.

state energy of the system can be obtained by diagonalizing the matrix described below:

$$H = \begin{pmatrix} \varepsilon_1 & H_{12} \\ H_{21} & \varepsilon_2 \end{pmatrix} \quad (1)$$

The potential energy functions of the diabatic valence bond states and their mixing term are represented by:

$$H_{ii} = \varepsilon_i = \alpha^i_{\text{gas}} + U^i_{\text{intra}}(R,Q) + U_{\text{Ss}}(R,Q,r,q) + U_{\text{ss}}(r,q) \quad (2)$$

where, α^i_{gas} is the gas-phase energy of the ith diabatic state, $U^i_{\text{intra}}(R,Q)$ is the intramolecular potential of the solute system, R and Q are vectors representing the atomic coordinates and charges of all the elements of a given state i, r and q are those of the surrounding protein and solvent, $U_{\text{Ss}}(R,Q,r,q)$ represents the interaction between the solute (S) atoms and the surrounding (s) solvent and protein atoms and finally $U_{\text{ss}}(r,q)$ corresponds to the potential energy of the protein/solvent system.

The off-diagonal elements are usually represented by:

$$H_{ij} = A_{ij}\mathrm{e}^{[-\mu_{ij}(r_{ab}-r_{ab,0})]} \quad (3)$$

Here, A_{ij} and μ_{ij} are empirical constants that are calibrated on the basis of the computational reproduction of the experimental free energy profile and r_{ab} represents the distance between the two atoms characterizing the ith and jth states of the affected bond. In addition, the H_{ij} elements are assumed to be the same in the gas phase, solution and protein.

In order to simulate the formation of the chemical bond during the transition between two EVB states, ε_1 and ε_2 (initial and final states), we conduct MD simulations of the system on a mapping potential, ε_m, that is determined by a linear combination of the initial and final states:

$$\varepsilon_m = (1 - \lambda_m)\varepsilon_1 + \lambda_m\varepsilon_2 \ (0 \le \lambda_m \le 1) \quad (4)$$

where, λ_m is an order parameter going from 0 to 1 in $N + 1$ windows as the initial state is changed to the final state. The free energy change between the consecutive steps can be calculated by the forward FEP procedure as:[16]

$$\Delta G_{m\to m+1} = -\beta^{-1}\ln\langle \mathrm{e}^{\{-\beta[\varepsilon_m(\lambda_{m+1})-\varepsilon_m(\lambda_m)]\}}\rangle_m \quad (5)$$

After MD-FEP calculations, the free energy functional that corresponds to the adiabatic ground state surface E_g was obtained by the FEP-umbrella sampling (FEP/US) method[16,17] that can be written as:

$$\Delta g(x') = \left\langle \sum_{m=0}^{i-1}\Delta G_{m\to m+1} - \beta^{-1}\ln\left\langle \delta(x-x')\mathrm{e}^{\{-\beta[E_g-\varepsilon_m(\lambda_i)]\}}\right\rangle_{\varepsilon_m}\right\rangle_i \quad (6)$$

where $\sum_{m=0}^{i-1}\Delta G_{m\to m+1}$ represents the free energy difference between the first and ith mapping potential, δ corresponds to Dirac's delta function. ε_m is the mapping potential that keeps x in the region of x'. The generated reaction coordinate, x, is usually taken as the energy gap ($x = \varepsilon_1 - \varepsilon_2$). This selection is particularly powerful when one tries to represent all of the many dimensional solvent space by a single coordinate. Additionally, it is important to note that the diabatic free energy profiles of the reactant and product represent the microscopic equivalent[18] of the Marcus parabolas.[19]

The LRA method

The linear response approximation (LRA) treatment[20,21] provides a good estimation for the free energy associated with the change between two potential surfaces (U_1 and U_2) by

$$\Delta G(U_1 \to U_2) = \tfrac{1}{2}(\langle U_2 - U_1\rangle_1 + \langle U_2 - U_1\rangle_2) \quad (7)$$

The notation $\langle\rangle_i$ designates an average over trajectories propagated on the potential energy surface U_i. Herein, we have used the LRA approach to calculate the free energy of changing the charges of a given state from actual EVB charges (Q) to the charges of the nonpolar state (zero residual changes). It is important to clarify that only electrostatic interactions were considered for evaluating the solvation free energy for both RS and TS, where vdW parameters within the uncharged state were kept identical to those within the charged state. Since we are interested in calculating the solvation energy for each fragment involved in the reaction ($SAM^+ + Cl^-$) we have constructed (only for charging process) a second EVB state with a minimum whose structure resembles the geometry of the TS. Recently, we have used this approach in order to have the minimum of EVB2 shifted to the position of the TS for paradynamics studies (for more details about the EVB2 shift see ref. 11).

The system

The initial structure for calculations was taken from the Protein Data Bank (PDB) with the 2Q6I PDB code,[1] which shows SalL-Y70T with SAM and Cl^-. In order to simulate the native structure, we have modeled the Tyr residue instead of Thr in position 70. The systems included the reacting fragments (Fig. S1, ESI†), the protein and explicit water molecules. The simulation systems were solvated using the surface constrained all atom solvent model (SCAAS).[22] Here, we have used a water sphere with a radius of 20 Å centered on the substrate and surrounded first by a 2 Å grid of Langevin dipoles, and then by a bulk solvent. Long-range electrostatic effects were treated using

the local reaction field (LRF) method. A cut-off of 10 Å was used for the calculation of long-range interactions. In addition, the free energy was obtained using the canonical (*NVT*) ensemble which can be generalized to the Gibbs free energy (*NPT*) and other thermodynamic ensembles. Hydrogen atoms were added using the MOLARIS-XG program package.[23,24]

Free energy perturbation mapping was performed in 41 frames of 20 ps length each for the movement along the reaction coordinate, using the SCAAS model, after the respective system underwent a 1500 ps relaxation run. All simulations were performed at 300 K using a 1 fs time step. In order to obtain reliable sampling, the simulations were repeated at least five times under different initial conditions (obtained from arbitrary points in the relaxation trajectory after the initial 1500 ps relaxation run) for each reacting system. Weak residue constraints of 0.3 kcal mol^{-1} $Å^{-2}$ were applied to region I (part of the system described by the EVB) that involves part of SAM and Cl^- (Fig. S1, ESI†). All EVB calculations were carried out by the MOLARIS-XG simulation program[23,24] using the ENZYMIX force field. It is important to clarify that region I has the same amount of atoms in water and protein, since we are assuming the fact that the reacting system is the same in the enzyme and solution, the number of EVB atoms resulted then to be 12. In this study, the reaction in water was studied using the MOLARIS-XG simulation package, where the system included the reacting fragments (Fig. S1, ESI†) plus explicit water molecules. In this case, we have also used a water sphere with a radius of 20 Å centered on the substrate and surrounded first by a 2 Å grid of Langevin dipoles. It is also important to point out that the EVB approach relies on calibration of empirical parameters to describe the energetics of a reference reaction solution. Once calibrated, the same parameters are used to describe the process in an enzyme active site. Herein, we calibrated the empirical parameters in order to reproduce the activation free energy for the reaction in solution obtained from the experimental value.[3] The specific EVB parameters used for calibrating the EVB model are described in the ESI† (Table S4).

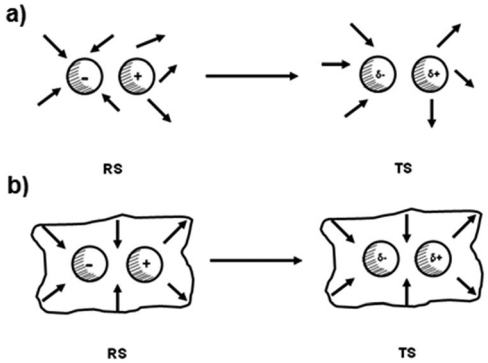

Fig. 2 Illustrating the dipoles in the S_N2 reaction studied (a) water and (b) protein active site environments. The dipoles are especially aligned (pre-organized) in proteins where the reorganization energy is lower than in water.

the enzyme[28,29] (see Fig. 2). In accordance with the electrostatic preorganization idea[10] the reduction of the activation barrier appears to result mainly from electrostatic interactions that 'solvate' the TS in the enzyme more effectively than the corresponding TS in solution.[21]

In this study, we calculated the activation barrier for the nucleophilic attack of Cl^- on a methyl group bonded to the sulfur atom of trimethylsulfonium, $(CH_3)_3S^+$, in aqueous solution and in the gas-phase using DFT,[30] HF[31] and MP2[32] levels of theory (see Table S1, ESI†). All quantum simulations were performed using Gaussian 09.[33] After the quantum mechanical calculations in the gas-phase, we have selected stationary points (reactants, transition state and products) in order to analyse the solvation effect of the methyl transfer reaction using the polarizable continuum model (CPCM),[34] where a single point calculation using 6-31+g(d,p) was carried out for each optimized geometry obtained from gas phase calculations. Interestingly, it was found that HF approximation provides the barrier calculated close to the experimental results obtained for the reaction in solution[3] (see Table S1, ESI†). Fig. 3 shows the free energy profile obtained from HF calculations

Results and discussion

Evaluating the reaction in water and the gas phase

According to the desolvation proposal, if an enzyme reaction takes place in the absence of water, then the reaction is catalyzed by an enzyme that is able to create an environment around reactants that is similar to the gas phase.[3,4] In other words, a nonpolar enzyme active site can catalyze reactions by desolvating reactants, where the destabilization of charged ground states can contribute to catalysis. In addition, experimental data[25] and calculations[26,27] have shown that reactions in the gas-phase involve a smaller activation barrier than the corresponding reactions in solution. Recently, Wolfenden and coworkers[3] have studied the catalysis of alkyl transfer from SAM to halide ions in solution. In their conclusion they have suggested that SAM dependent halide alkylating enzymes catalyze their reaction by desolvation. On the other hand, Warshel and coworkers have indicated that the catalytic effect of enzymes is mainly due to the optimal orientation of the permanent dipoles of

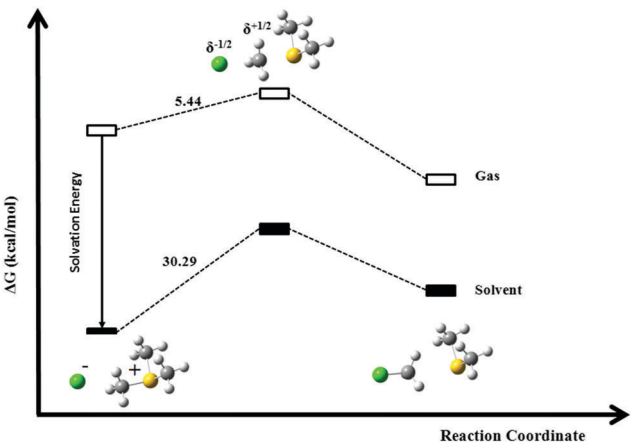

Fig. 3 Energy profile obtained from HF/6-31+(d,p) for the S_N2 reaction. The calculations were performed in water and the gas-phase for methyl transfer from trimethylsulfonium to chloride, where the chloride ion, carbon, sulfur and hydrogen atoms are depicted in green, gray, yellow and white, respectively.

for the nucleophilic attack of Cl^- on the methyl group of $(CH_3)_3S^+$. The results depicted in Fig. 3 suggest that activation free energy for the reaction studied in solution is higher than for the reaction in the gas-phase. In this sense, one could suggest that the reaction in an enzyme environment has a lower activation barrier, just like the analogous reaction in the gas-phase (Fig. 3). Indeed, there are reactions accelerated by moving from polar to nonpolar solvents.[35] However, reactions in nonpolar solvents are not the same as reactions in the active sites of an enzyme which is surrounded by a polar solvent. In addition, it is important to emphasize that the only way to test desolvation proposal is evaluating the binding energies of RS and TS in the protein and aqueous solution. Besides, analyzing only energetic diagrams (Fig. 3) for reactions in water and the gas-phase cannot provide the answers about the catalysis in the enzyme active sites, where there are key intermolecular interactions between the substrate and catalytic residues.

Evaluating the reaction in water and proteins

Despite significant advances in computational power, the use of a higher-level quantum mechanical approach remains cumbersome for modeling reactions in proteins, particularly if one is interested in obtaining convergent free energies.[36] This problem is circumvented by the EVB[15] which is a semi-empirical method used to describe bond-breaking and bond-making processes.[36] The EVB surface of proteins is calibrated using the experimental information for the reaction in aqueous solution which allowed us to explore the free energy surface in the chlorinase without the challenge of obtaining fully converging QM(*ai*)/MM. Therefore, using the reported values for the reaction in water[3] (34.50 kcal mol^{-1}) we obtain $\Delta g^{\ddagger}_{cage} = 32.0\,kcal\,mol^{-1}$ for the reaction in solution, considering the fact that the free energy costs of bringing the reacting fragment to the same solvent cage is around 2.5 kcal mol^{-1}.[8,9] For the reaction catalyzed by the native chlorinase[1] we obtained $\Delta g^{\ddagger}_{cat} = 20.12\,kcal\,mol^{-1}$ from the experimental data.[1] The calculated activation energy for reactions in water and in the chlorinase is compared to the corresponding observed values described above summarized in Table 1. The calculated activation free energies for reactions in the protein and water are in a reasonable agreement with the corresponding experimental values. The free energy profiles for reactions in the enzyme and aqueous solution are presented in Fig. 4. To explore the source of the large enhancement produced by chlorinase, we have calculated the electrostatic energies of the RS and TS in both the protein and water environments. In the reaction studied here, the charge distributions change from localized charge at the RS to delocalized charge at the TS, where we have +1 (SAM^+), −1 (Cl^-) for the RS and +0.73, −0.73 for the TS (Mulliken charges for the reaction in solution). In this sense, it would be difficult for the enzyme dipole to solvate the TS more than the RS and it would be even more difficult to obtain sufficient solvation by the solvent dipoles in the reference reaction.

Table 1 Activation free energies for the S_N2 step of the methyl transfer reaction in the chlorinase and solution[a] obtained from EVB/MM calculations

	$\Delta g^{\ddagger}_{calc}$ (kcal mol^{-1})	$\Delta g^{\ddagger}_{exp}$ (kcal mol^{-1})
Water cage (SAM)	32.0	34.50[b]
Native	20.12 (±0.10)	20.07[c]
Y70T	22.65 (±0.77)	24.41[c]

[a] The free energy perturbation mapping was performed with 41 frames of 20 ps each, for the movement along the reaction coordinate. [b] Results obtained by Lohman, Edwards and Wolfenden, 2013.[3] [c] Results obtained by Eustáquio and co-workers, 2008.[1]

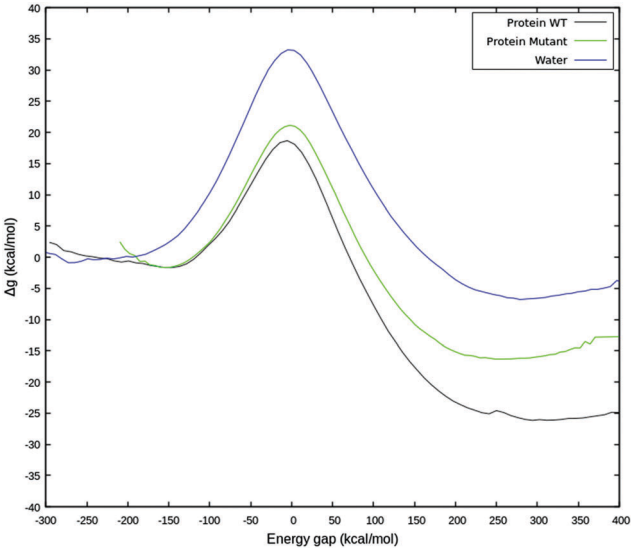

Fig. 4 The actual adiabatic free energy profile for the S_N2 reference reaction in water and in chlorinase native and its Y70T mutant. Note that the values reported in Table 1 are average of activation energy obtained from different free energy surfaces. Here is depicted one of these FESs.

The solvation energies of the RS and TS in the protein and in water were calculated using the LRA approach. The electrostatic interactions between the substrate and its surrounding for RS and TS are depicted in Table 2, where $\langle U_Q - U_0\rangle_Q$ correspond to trajectories where the substrate charges exist for the environment and $\langle U_Q - U_0\rangle_0$ correspond to trajectories where the substrate charges do not exist for the environment. As can be seen from Table 2, the protein solvates the RS more than water does, taking the sum of the solvation energy for each RS fragment into consideration. In addition, in accordance with the results depicted in Table 2, the solvation energy for chloride ions is critical for the RS electrostatic stabilization which is inconsistent with the desolvation proposal. It is important to emphasize that the enzyme provides a pre-organized dipolar environment that is already partially oriented so as to stabilize the charge distribution in the TS. In reactions in water, orienting the polar environment towards the TS charges requires significant reorganization energy. Warshel proposed that in polar solvents about half of the energy gained from charge–dipole interactions is spent on changing the dipole–dipole interaction, $G_{\mu\mu}$, so that the free energy of solvation of the transition state is given by the following equation:[35]

$$\Delta G_{sol} \cong \Delta G_{Q\mu} + \Delta G_{\mu\mu} \cong \Delta G_{Q\mu} - 1/2\Delta G_{Q\mu} = 1/2\Delta G_{Q\mu} \quad (8)$$

where $G_{Q\mu}$ is the actual electrostatic interaction between the environment (protein or water) and the substrate. In the protein environment, the dipoles are already partially oriented

Table 2 The solvation free energies (kcal mol^{-1}) of the RS and the TS in the reference reaction in water and the catalytic reaction in chlorinase[a]

	Protein WT		Mutant		Water	
	RS (Cl^-)	TS ($Cl^{-1/2}$)	RS (Cl^-)	TS ($Cl^{-1/2}$)	RS (Cl^-)	TS ($Cl^{-1/2}$)
$\langle U_Q - U_0\rangle_Q$	−130.06 (±0.1)	−109.68 (±2.3)	−136.62 (±1.7)	−112.95 (±3.5)	−155.08	−120.01
$\langle U_Q - U_0\rangle_Q$	−43.51 (±2.9)	−25 (±0.1)	−40.79 (±2.5)	−11.36 (±1.9)	10.43	39.6
ΔG_{solv}	−86.78 (±1.4)	−67.34 (±1.1)	−88.7 (±2.1)	−62.16 (±3.1)	−72.33	−40.21
$\Delta\Delta G^{\ddagger}_{solv}$	19.44	26.54	32.12			

[a] The energies were obtained through the LRA approach using the charged system as state I and the uncharged system as state II. We have used the shifted EVB approach for computing the solvation energy for the TS, see ref. 19 for more details about shifted EVB.

toward the transition state charge center.[35] Thus, $\Delta G_{\mu\mu}$ is smaller than in water, and less free energy is spent on creating the oriented dipoles of the protein transition state.

Analyzing the reaction in the Y70T mutant

We also evaluated the catalytic effect of Y70T mutation in chlorinase. Eustáquio and co-workers[1] have reported kinetic parameters for the formation of 5′-ClDA and L-methionine in the chlorinase Y70T mutant, using their reported value, we estimated $\Delta g^{\ddagger}_{exp} = 24.4\,kcal\,mol^{-1}$ for the reaction catalyzed by this protein mutant. In accordance with the desolvation idea the polarity of the native enzyme active sites would be less effective than in its Y70T mutant because active site residues desolvate the reacting fragments and thus improve the catalytic efficiency in native. However, in accordance with our computational simulations we note that the difference in the catalytic effect of the native and mutant is almost entirely due to the difference in the electrostatic contribution to the activation barrier. Here the electrostatic stabilization of Cl^- in the RS and TS in the native is larger than in the mutant enzyme and this leads to a larger activation barrier in the mutant. Therefore, the polarity of the native enzyme active sites is more effective in native than in its Y70T mutant which implies that desolvation cannot enhance the rate of reaction for native, since the native solvates better Cl^- than the mutant does. Chlorinase Y70T mutation increases g which is supported by the idea that preoriented dipoles in an enzyme can account for catalysis. It is important to note that solvation energies of the RS and TS can be obtaining by the sum of the solvation energies of the reacting fragment ($SAM^+ + Cl^-$). In this case, the results show that calculated activation energy ($\Delta\Delta G^{\ddagger}_{solv}$) for native, mutant and water corresponds to $\Delta\Delta G^{\ddagger}_{solv} = 34.2$, $\Delta\Delta G^{\ddagger}_{solv} = 52.4$ and $\Delta\Delta G^{\ddagger}_{solv} = 52.2\,kcal\,mol^{-1}$, respectively (see Table S5, ESI†). In fact, the effect of the mutation is overestimated when SAM^+ is taken into account (see Table S5, ESI†). However, it is also important to mention that due to the size of SAM^+, the changes in solvation energy for this cation are lower than for Cl^- (see Table S5, ESI†). It is likely that much more extensive sampling would improve the results for the mutational effect. However, this is not the purpose of the present work. Here, we have focused on the results obtained for the chloride anion.

It is worth mentioning that there are more apolar residues present in the active sites of chlorinase than polar residues (see Fig. 5). Despite the apolar character inside the pocket of chlorinase. The key residues are positioned in order to create an optimal electrostatic environment for stabilizing the negative charge of chloride ions. For example, Gly131 is an apolar residue. On the other hand, chloride ions form hydrogen bonds with the amide backbone of Gly131 (2.8 Å) as well as an internal water molecule and a threonine residue in the active sites of chlorinase (see Fig. 6). Interestingly, experimental data show that replacement of Gly131 with a serine led to the loss of SalL halogenase activity.[1] Despite that, chlorinase acts on its substrates without assistance of metals or polar residues. This

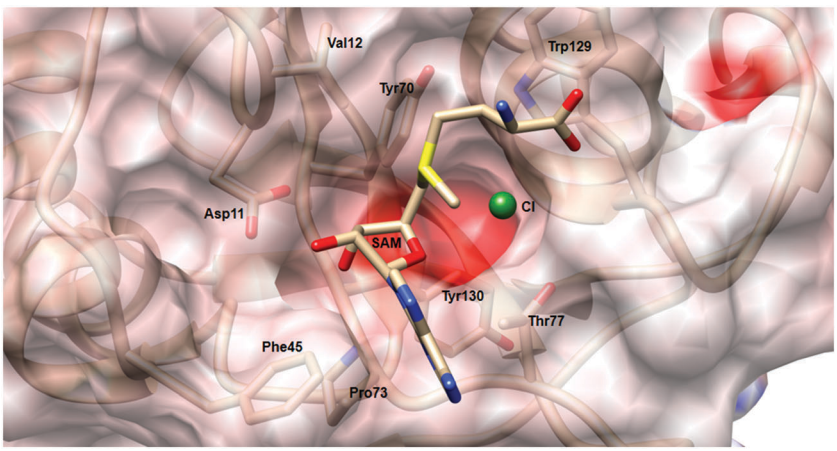

Fig. 5 Electrostatic surface representation of the chlorinase active sites.

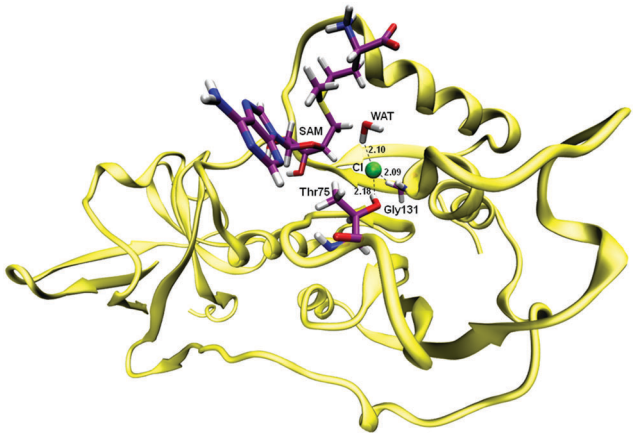

Fig. 6 The chlorinase in complex with SAM and Cl^-. Hydrogen bond between chloride (in green) and key residues in the active sites of this enzyme. Despite there are more apolar than polar residues present in the active sites of this enzyme, chloride ions form hydrogen bonds with the key residue in its active sites.

enzyme uses key active site interactions that optimally stabilize the transition state during the reaction. In the case of chlorinase, strong hydrogen bond interactions between Gly131 and Cl^- and pre oriented dipoles in its active sites are sufficient to account for the rate enhancements achieved by this enzyme that manages to stabilize the system by hydrogen bonds (dipoles) which are especially aligned towards the negatively charged chloride. Therefore, our computational results did not find that SAM dependent halide alkylating enzymes catalyze their reaction by the desolvation of Cl^- in the active sites of chlorinase. We found here that in the related case of chlorinase Cl^- is more stable in the enzyme than in water. Thus, the catalytic effect of chlorinase appears to result mainly from electrostatic interactions that "solvate" Cl^- in the enzyme more effectively than in solution which is in agreement with the electrostatic idea.[28]

Conclusion

In principle, desolvation proposal and the electrostatic preorganization effect cannot be evaluated without computational modeling. Here, we have addressed the main point raised in a recent experimental study that has proposed that SAM dependent halide alkylating enzymes catalyze their reaction through a desolvation mechanism. Desolvation proposal suggests that enzymes work by moving polar or charged reacting fragments to a non-polar environment and thus destabilizing the ground state. However, in the case of the reaction catalyzed by chlorinase, we found that the RS is more stable in the enzyme than in water and that thus the desolvation idea does not apply to catalysis of alkyl transfer from SAM to halide ions. In fact, it is well known that a nonpolar solvent can accelerate S_N2 reactions. However, only the observation that some reactions are accelerated upon moving from polar to nonpolar solvents cannot support the idea that an enzyme accelerates its catalysis reaction by resembling the corresponding gas-phase reaction. It is important to point out that substrates make key intermolecular interactions with residues in the active sites of enzymes and such interactions stabilize the RS. Furthermore, the difference between the solvation free energy of the RS and TS is smaller in the protein ($\sim$19 kcal mol^{-1}) than in the water solution ($\sim$32 kcal mol^{-1}), which explains the large catalytic effect in the enzyme, where there is a preferential stabilization of the less-polar TS. Our results also show that chlorinase solvates Cl^- more than water does, which is critical for the RS and TS electrostatic stabilization. In summary, the analysis described in this manuscript indicates that SAM-dependent chlorinase does not use the desolvation mechanism, but provides the electrostatic stabilization of chloride ions necessary for catalysis.

Acknowledgements

This work was supported by grant 441922/2014 of the Conselho Nacional de Desenvolvimento Científico e Tecnológico (CNPq). We gratefully acknowledge the University of Southern California's High Performance Computing and Communications Center for computer time. J. L. thanks the Professor Arieh Warshel for many important discussions about chemical reactions in enzymes.

References

1 A. S. Eustáquio, F. Pojer, J. P. Noel and B. S. Moore, *Nat. Chem. Biol.*, 2008, **4**, 69.
2 R. H. Feling, G. O. Buchanan, T. J. Mincer, C. A. Kauffman, P. R. Jensen and W. Fenical, *Angew. Chem., Int. Ed.*, 2003, **42**, 355.
3 D. C. Lohman, D. R. Edwards and R. Wolfenden, *J. Am. Chem. Soc.*, 2013, **135**, 14473.
4 M. J. Dewar and D. M. Storch, *Proc. Natl. Acad. Sci. U. S. A.*, 1985, **82**, 2225.
5 R. Wolfenden, *Science*, 1983, **222**, 1087.
6 A. Warshel, J. Aqvist and S. Creighton, *Proc. Natl. Acad. Sci. U. S. A.*, 1989, **86**, 5820.
7 J. Lameira, R. P. Bora, Z. T. Chu and A. Warshel, *Proteins: Struct., Funct., Bioinf.*, 2015, **83**, 318.
8 M. H. M. Olsson and A. Warshel, *J. Am. Chem. Soc.*, 2004, **126**, 15167.
9 A. Warshel and W. W. Parson, *Dynamics of biochemical and biophysical reactions: insight from computer simulations*, 2001, vol. 34.
10 A. Warshel, P. K. Sharma, M. Kato, Y. Xiang, H. Liu and M. H. M. Olsson, *Chem. Rev.*, 2006, **106**, 3210.
11 J. Lameira, I. Kupchencko and A. Warshel, *J. Phys. Chem. B*, 2016, **120**, 2155.
12 A. H. Lima, C. N. Alves, R. Prasad and J. Lameira, *Mol. BioSyst.*, 2016, **12**, 2980.
13 N. de Farias Silva, J. Lameira, C. N. Alves and S. Martí, *Phys. Chem. Chem. Phys.*, 2013, **15**, 18863.
14 J. R. A. Silva, T. Govender, G. E. M. Maguire, H. G. Kruger, J. Lameira, A. E. Roitberg and C. N. Alves, *Chem. Commun.*, 2015, **51**, 12560.

15 A. Warshel and R. M. Weiss, *J. Am. Chem. Soc.*, 1980, **102**, 6218.
16 A. Warshel, *Computer modeling of chemical reactions in enzymes and solutions*, John Wiley & Sons, New York, 1991.
17 J. Aaqvist, A. Warshel and J. Aqvist, *Chem. Rev.*, 1993, **93**, 2523.
18 G. King and A. Warshel, *J. Chem. Phys.*, 1990, **93**, 8682.
19 R. A. Marcus, *J. Chem. Phys.*, 1965, **43**, 679.
20 F. S. Lee, Z. T. Chu, M. B. Bolger and A. Warshel, *Protein Eng.*, 1992, **5**, 215.
21 A. Warshel, P. K. Sharma, M. Kato and W. W. Parson, *Biochim. Biophys. Acta, Proteins Proteomics*, 2006, **1764**, 1647.
22 A. Warshel and G. King, *Chem. Phys. Lett.*, 1985, **121**, 0–5.
23 F. S. Lee, Z. T. Chu and A. Warshel, *J. Comput. Chem.*, 1993, **14**, 161.
24 A. Warshel, Z. T. Chu, J. Villa, M. Strajbl, C. N. Schutz, A. Shurki, S. Vicatos, S. Chakrabarty, N. V. Plotnikov and P. Schopf, *MOLARIS-XG*, University of Southern California, Los Angeles, 2012.
25 A. Warshel and S. Russell, *J. Am. Chem. Soc.*, 1986, **108**, 6569.
26 S. J. Weiner, G. L. Seibel and P. A. Kollman, *Proc. Natl. Acad. Sci. U. S. A.*, 1986, **83**, 649.
27 S. Scheiner, D. A. Kleier and W. N. Lipscomb, *Proc. Natl. Acad. Sci. U. S. A.*, 1975, **72**, 2606.
28 A. Warshel, *Proc. Natl. Acad. Sci. U. S. A.*, 1978, **75**, 5250.
29 A. Warshel, P. K. Sharma, M. Kato, Y. Xiang, H. Liu and M. H. M. Olsson, *Chem. Rev.*, 2006, **106**, 3210.
30 P. Hohenberg and W. Kon, *Phys. Rev. B: Condens. Matter Mater. Phys.*, 1964, **136**, 864.
31 C. C. J. Roothaan, *Rev. Mod. Phys.*, 1951, **23**, 69.
32 M. Head-Gordon, J. A. Pople and M. J. Frisch, *Chem. Phys. Lett.*, 1988, **153**, 503.
33 M. J. Frisch, G. W. Trucks, H. B. Schlegel, G. E. Scuseria, M. A. Robb, J. R. Cheeseman, V. B. G. Scalmani, B. Mennucci, G. A. Petersson, H. Nakatsuji, C. Caricato, X. Li, H. P. Hratchian, A. F. Izmaylov, J. Bloino, G. Zheng, J. L. Sonnenberg, M. Had and D. J. Fox, *Gaussian 09, Revision A.02*, Gaussian, Inc., Wallingford CT, 2009.
34 V. Barone and M. Cossi, *J. Phys. Chem. A*, 1998, **102**, 1995.
35 A. Warshel, *J. Biol. Chem.*, 1998, **273**, 27035.
36 A. Shurki, E. Derat, A. Barrozo and S. C. L. Kamerlin, *Chem. Soc. Rev.*, 2015, **44**, 1037–1052.

